ACS APPLIED MATERIALS & INTERFACES

Research Article

www.acsami.org

Cooperative Assembly of Pyrene-Functionalized Donor/Acceptor Blend for Ordered Nanomorphology by Intermolecular Noncovalent $\pi-\pi$ Interactions

Lie Chen,[†] Siwan Peng,[†] and Yiwang Chen*[,†,‡]

[†]Institute of Polymers/Department of Chemistry, Nanchang University, 999 Xuefu Avenue, Nanchang 330031, China

[‡]Jiangxi Provincial Key Laboratory of New Energy Chemistry, Nanchang University, 999 Xuefu Avenue, Nanchang 330031, China

Supporting Information

ABSTRACT: A facile approach to develop the stable and well-defined bulk heterojunction (BHJ) nanomorphology has been demonstrated. Novel pyrene (Py)-functionalized diblock copolymers poly(3-hexylthiophene)-*block*-poly[3-(10-(pyren-1-yloxy)decyloxy)thiophene] (P3HT-*b*-P3TPy), and pyrene-functionalized fullerene [6,6]-phenyl-C_{61}-butyric acid 1-pyrene butyl ester (PCBPy), were successfully synthesized. The $\pi-\pi$ interactions of Py mesogens interdigitated between the functionalized fullerene and P3TPy segment can allow for the cooperative assembly of P3HT-*b*-P3TPy and PCBPy. The orientation of the Py mesogens also can further enhance the molecular arrangement. Compared with the as-cast and thermal annealing, solvent annealing can promote cooperative assembly of P3HT-*b*-P3TPy:PCBPy undergoing the slow film growth. Note that the assembly microstructure strongly depends on the molar ratio of P3HT and P3TPy with Py mesogens. Low loading of P3TPy block in the copolymers blends keeps the same behavior to the P3HT, whereas relatively high loading of Py mesogens favors the better intermolecular $\pi-\pi$ stacking interactions between P3HT-*b*-P3TPy and PCBPy. As a result, the P3HT-*b*-P3TPy(3/1) forms the orientated nanowires with PCBPy in bulk heterojunction, and the average domain size is estimated to be 10−20 nm, which is desirable for enlarge surface area for donor/acceptor interfaces and give a bicontinuous pathway for efficient electron transfer. Furthermore, the cooperative assembly between P3HT-*b*-P3TPy and PCBPy is found to effectively suppress the PCBPy macrophase separation, and stabilize the blend morphology.

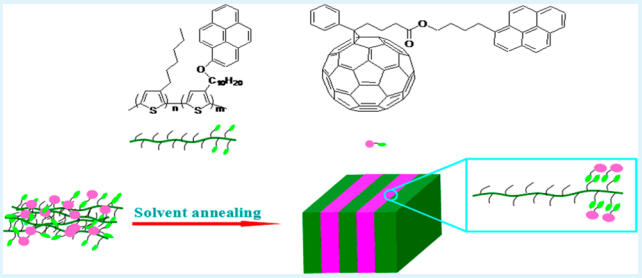

KEYWORDS: *nanowires, cooperative assembly, morphology, diblock copolymers*

INTRODUCTION

Conjugated polymer-based bulk heterojunction (BHJ) photovoltaic devices have received strong interest for the past few years with the urgent need of lightweight, flexible, low-cost solar cells.[1−3] The photoactive layer of BHJ solar cells is consisting of a blend of conjugated polymers as the electron donor and fullerene derivatives as the electron acceptor, which is capable of forming the interpenetrated networks and introducing a large interfacial area for effective exciton dissociation.[4−6] The blend systems of poly(3-hexylthiophene) (P3HT) and [6,6]-phenyl C_{61}-butyric acid methyl ester (PCBM) is one of the most widely studied active layer. To date, the power conversion efficiency (PCE) of polymer solar cells based on P3HT/PCBM systems has reached to 4−5%.[7,8]

As we all know, the nanomorphology of the photoactive layer is one of the key factors to impact on the efficiency and stability of the BHJ. Because of the limited exciton diffusion length of the organic materials (ca. 10 nm),[9,10] highly ordered nanostructured morphologies, which have large interfaces and a bicontinuous pathway, are expected for the photoactive layer. Various approaches like thermal annealing,[11,12] solvent annealing[13,14] and additives[15] are applied to achieve the large D/A interface and small-sized domains for efficient exciton dissociation and charge generation. However, the network structure of P3HT:PCBM can not give a bicontinuous pathway for electrons and holes to transfer toward the corresponding electrodes, and the extensive isolated domains by the crystallization of PCBM are often observed. Thus, it is desirable to find effective methods for controlling and achieving a stable well-ordered morphology.

Recently, conjugated block copolymers (BCPs) consisting of two or more chemically distinct chains covalently linked at one end have been identified as a promising photoactive materials in BHJ solar cell devices, which are able to self-assemble on length scales from a few to hundreds of nanometers, comparable to the exciton diffusion length. Meaningfully, McCullough and co-workers[16,17] have discovered the one-pot synthesis of diblock conjugated polymer with high molecular weights and narrow polydispersities by the Grignard metathesis (GRIM) method. Up to now, the mostly synthesis of block

Received: January 22, 2014
Accepted: May 21, 2014
Published: May 21, 2014

   dx.doi.org/10.1021/am501831z | ACS Appl. Mater. Interfaces 2014, 6, 8115−8123

Scheme 1. Synthesis of Diblock Copolymers P3HT-b-P3TPy

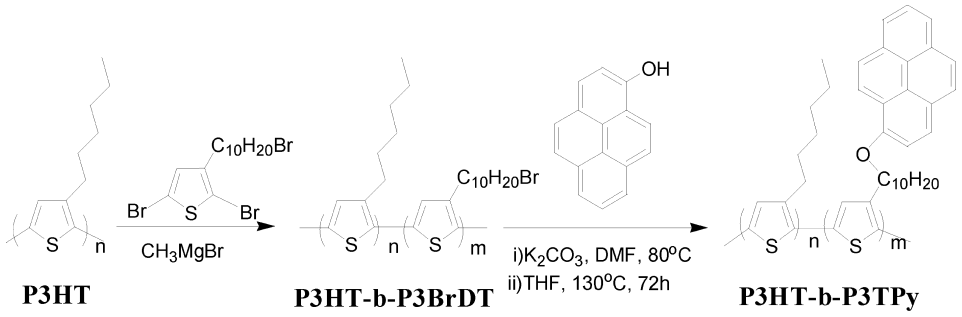

P3HT-b-P3TPy(3/1), n:m=3:1
P3HT-b-P3TPy(10/1), n:m=10:1
P3HT-b-P3TPy(14/1), n:m=14:1

copolymers with regioregular poly(3-hexylthiophene) (P3HT) as the conjugated block can self-assemble into a relatively ordered lamellar semicrystalline phase to possess a high hole mobility.[18−20] To control the nanoscale microphase saperation and morphological stability, noncovalent or covalent interactions between the donor and acceptor are introduced.[21−29] Wudl et al.[21] reported on the synthesis of a rod−coil triblock copolymer, P3HT-*b*-P(S_{89}BAz_{11})-C_{60}, via covalently linking the P3HT and C_{60}, and nanofibrilar structure has been successfully achieved. However, it is extremely challenging to synthesize block copolymers that possess high ratios of fullerene groups via the covalently bound. On the other hand, the strong noncovalent, such as hydrogen bonding, could construct higher-order supramolecules by cooperative assembly of the acidulated fullerene molecules and functionalized polythiophene.[22−24] Zhu et al.[25,26] reported on an interesting method to construct supramolecular assembly between the uracil-functionalized donor and 2,6-diaminopyridine-functionalized acceptor by a three-point hydrogen bonding. By these approaches, the compatibility of components and the D/A interface area can be greatly enhanced, consequently resulting in more efficient exciton dissociation and charge generation. However, the ordering degree of the separated nanophase is difficult to precisely control, which limits the charge carriers transporting to their corresponding electrodes.

In our previous work,[30] we have reported a diblock copolymer bearing discotic liquid crystals moiety, poly(3-hexylthiophene)-*block*-poly[3-(10-(2,3,6,7,10-pentakis-(hexyloxy)triphenylen)-decyloxy)thiophene] (P3HT-*b*-P3TPT). The diblock copolymer could easily self-assemble into nanowire structure by tuning P3HT:P3TPT block ratio and employing different annealing process. More importantly, the orientation of mesogens could well induce the diblock copolymers to pack with more ordered arrangement. However, because of lack of the interaction between the copolymer donor and fullerene acceptor, a favorable microphase nanomorpology was not obtained by simply blend the P3HT-*b*-P3TPT with PCBM. In this work, novel pyrene (Py) mesogen functionalized diblock polythiophene and fullerene, namely poly(3-hexylthiophene)-*block*-poly[3-(10-(pyren-1-yloxy)decyloxy)thiophene] (P3HT-*b*-P3TPy) and [6,6]-phenyl-C_{61}-butyric acid 1-pyrene butyl ester (PCBPy), respectively, are prepared. The $\pi-\pi$ interactions of Py groups[31] between the functionalized fullerene and P3TPy segment can promote the cooperative assembly of P3HT-*b*-P3TPy and PCBPy, and the orientation of the Py mesogens also can further enhance the molecular arrangement. Therefore, a desirable BHJ nanostructure is anticipated, which can enlarge surface area for donor/acceptor interfaces and give a bicontinuous pathway for efficient electron transfer. On the other hand, due to the strong interaction between the P3HT-*b*-P3TPy and PCBPy by incorporation of Py mesogens, the macrophase aggregation could be greatly suppressed to improve the BHJ morphological stability. The assembled nanostructures are investigated by X-ray diffraction (XRD), atomic force microscopy (AFM) and transmission electron microscopy (TEM), and the effect of P3TPy block ratio on the morphology and its stability has also been given a special attention.

RESULTS AND DISCUSSION

Scheme 1 shows the synthesis of target diblock copolymers P3HT-*b*-P3TPy (more detailed information in Scheme S1 in the Supporting Information). The regioregular P3HT block was first prepared by GRIM method (using Ni(dppp)Cl_2) to give P3HT with a living chain-end, followed by chain extension with different feed ratios of activated 2-bromo-3-(10-bromodecyl)-5-magnesium bromodithiophene monomer, to obtain the medium diblock copolymers poly(3-hexylthiophene)-*b*-poly(3-(10-bromodecyl)thiophene)(P3HT-*b*-P3BrDT). In copolymers P3HT-*b*-P3BrDT, the bromide groups were completely substituted via Williamson ether reaction by 1-hydroxypyrene (^{1}H NMR spectroscopy in Figure S1 in the Supporting Information), which was prepared according to the methods described in the literature,[32] to give the resulting copolymers P3HT-*b*-P3TPy. All copolymers were purified by sequential Soxhlet extraction using methanol, hexane, and chloroform in succession. ^{1}H NMR spectra of copolymers P3HT-*b*-P3BrDT and corresponding polymer P3HT-*b*-P3TPy are shown in Figure 1, respectively. The signal (3.40 ppm) in spectrum of P3HT-*b*-P3BrDT is evident from the protons on the methylene for Br (CH_2−Br), while the signal (4.10 ppm) in spectrum of P3HT-*b*-P3TPy is assigned to methylene for oxygen (CH_2−O). It confirms that all of the bromine atoms were converted to Py moieties during the substitution reaction. Three ultima diblock copolymers had different targeted P3HT:P3TPy molar ratios of 3:1, 10:1 and 14:1, denoted P3HT-*b*-P3TPy(3/1), P3HT-*b*-P3TPy(10/1), P3HT-*b*-P3TPy(14/1), respectively. The actual block ratios (molar monomer equivalent) were calculated by comparing the signal intensity of the methylene group (adjacent to the

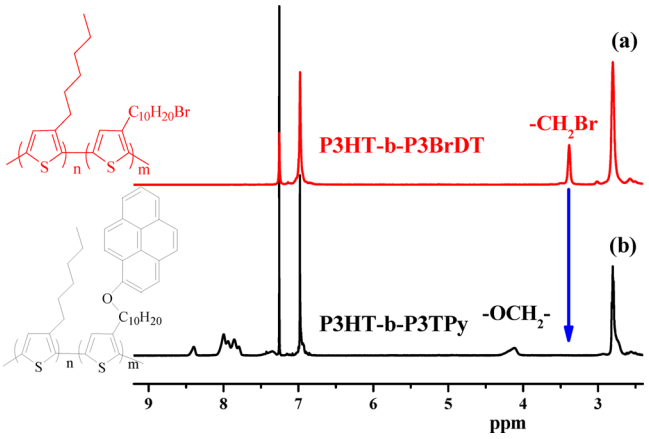

Figure 1. ^{1}H NMR spectra of (a) P3HT-*b*-P3BrDT and (b) P3HT-*b*-P3TPy after complete substitution by the pyrene group.

thiophene ring) at 2.80 ppm to the methylene group (adjacent to the oxygen atom) at 4.10 ppm in ^{1}H NMR spectroscopy (details in Figure S2 in the Supporting Information). These block copolymers exhibit good solubility in common solvent such as chloroform and tetrahydrofuran. Gel permeation chromatography (GPC) measurements were done to calculate their molecular weights by using tetrahydrofuran as the eluent. And the M_w, polydispersity (PDI) and GPC curves have been shown in Figure S3 in the Supporting Information. All three of the diblock polymers have high molecular weights and very narrow PDI.

The synthesis of fullerene derivative PCBPy is shown in Scheme 2. PCBPy was successfully obtained from the esterification reaction of PCBA and 1-pyrenebutanol. As can be seen from the ^{1}H NMR (see Figure S4 in the Supporting Information) spectrum of PCBPy, two obvious resonance peaks appear at 7.5−8.3 and 4.2, associated with the proton of the pyrene ring and methylene for oxygen (CH_2−O), respectively. The PCBPy also exhibits excellent solubility in chloroform, tetrahydrofuran, chlorobenzene, and orthodichlorobenzene (oDCB).

P3HT-*b*-P3TPy is blended with PCBPy with the weight ratio of 1:1, which is generally regarded as the optimized weight ratio of P3HT:PCBM based solar cells. Through the $\pi-\pi$ interaction of Py mesogens between the P3TPy segments and PCBPy, the PCBPy is expected to preferentially cooperative self-assemble with the P3TPy domains. Different treatments including as-cast, thermal annealing (TA) at 150 °C for 30 min, oDCB solvent annealing (SA) for 1 h were performed on the blend films. The temperature of thermal annealing has been set as 150 °C, which is found to be the optimal option after the comparison of different annealing temperatures. Figure 2 shows the UV−visible absorption spectra of the P3HT-*b*-P3TPy as-cast thin films and their blends with PCBPy after various annealing treatment (see details in the Supporting Information). From Figure 2a, we can see that absorption spectra of three different ratios as-cast P3HT-*b*-P3TPy thin films are almost identical. They all exhibit three peaks at 520, 560, and 610 nm, respectively, which are the characteristic absorption bands of P3HT, indicating that the P3TPy block does not affect the conjugation length of the P3HT block. The absorption shoulder at 610 nm has been reported to be indicative of the strong polythiophene interchain interaction, therefore it suggests the copolymers remain the high degree of crystallinity in P3HT, despite the presence of the P3TPy segment. In the ultraviolet region around 350−385 nm, the absorption band is attributed to $\pi-\pi^*$ transition of the Py moiety,[31] and the intensity of the absorption shoulder peak is proportional to the ratios of the Py moiety. After being blended with PCBM with the weight ratio of 1:1, the P3HT-*b*-P3TPy(14/1):PCBM film shows the similar behavior to the P3HT:PCBM (w:w = 1:1) film, in which the thermal treatment could increase the interchain interaction and strengthen crystallinity of the P3HT block as evidenced by the enhanced shoulder intensity at 610 nm (see Figure S5b in the Supporting Information). With the content of Py moiety increasing, both TA and SA exert little influence on the shoulder intensities of P3HT-*b*-P3TPy(10/1) and P3HT-*b*-P3TPy(3/1), probably because too much bulky Py mesogens in the copolymer films is not beneficial for the arrangement of polymer chains (see Figure S5c, d in the Supporting Information). Interestingly, if the copolymer P3HT-*b*-P3TPy is blended with mesogen-modified PCBPy, followed by SA, the interaction between P3HT-*b*-P3TPy and PCBPy can induce the films arranged with more ordered nanostructure. As shown in Figure 2b−d, compared to the thermal annealing process, the solvent annealing can prolong the film growth and enable the molecules to arrange with higher crystallinity, thus the more ordered structure causes a significant red-shift in their absorption edge, together with a relative higher intensity of the absorption shoulder peak. However, the direct thermal annealing (TA) can not serve the same function on all the blends of the P3HT-*b*-P3TPy/PCBPy compared to SA. This may be because thermal annealing process results in relative fast film growth, and therefore the bulky mesogen makes it hard to promote the original arrangement of polymer chains and develop less ordered nanostructures with lower crystallinity.

To probe into it adequately, we also investigated the photoluminescence. The fluorescence spectra of as-cast films of the P3HT-*b*-P3TPy block copolymers, and of their blends with PCBM or PCBPy produced by excitation with the 520 nm, are represented in Figure S6 in the Supporting Information and Figure 3, respectively. From them, we can see that a strong decrease in luminescence intensity can be seen on the all blend films under thermal or solvent annealing treatments compared

Scheme 2. Synthesis of Fullerene Derivative PCBPy

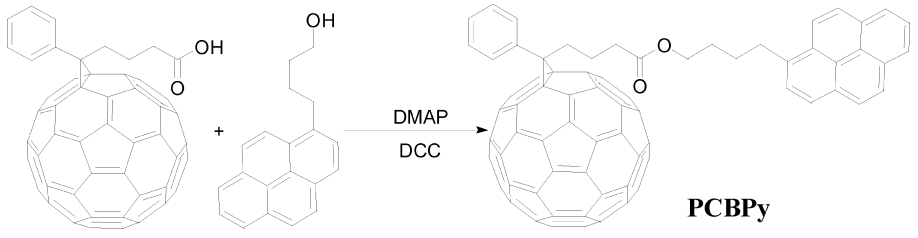

dx.doi.org/10.1021/am501831z | ACS Appl. Mater. Interfaces 2014, 6, 8115−8123

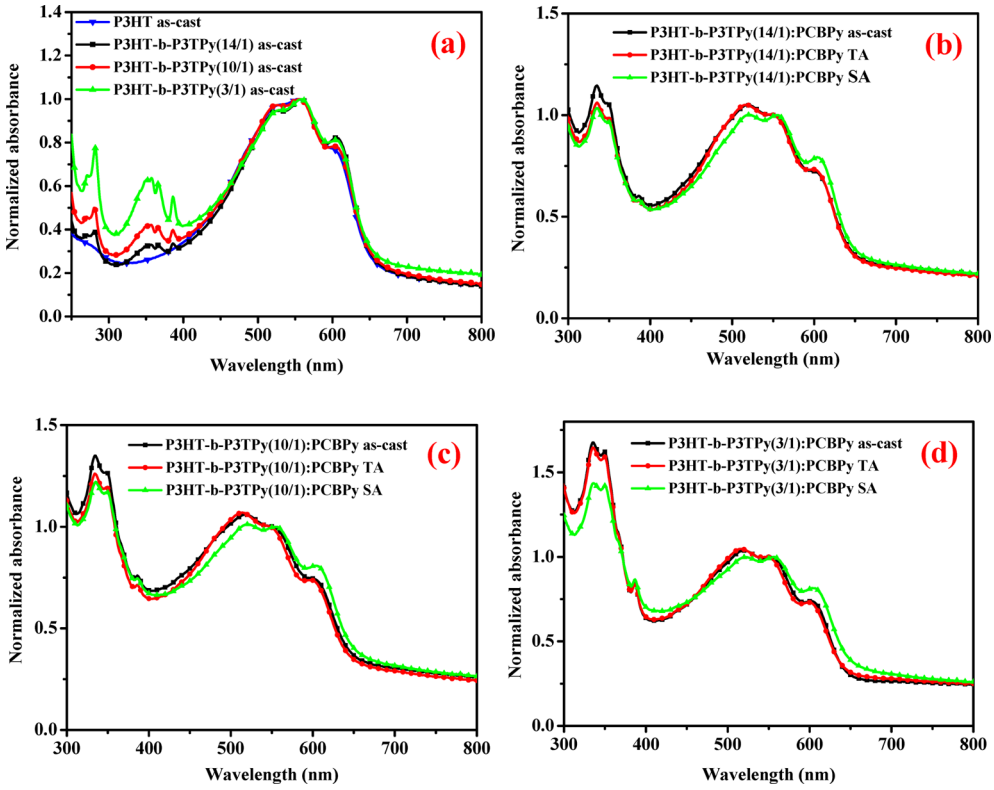

Figure 2. UV−vis spectra of films of (a) pure P3HT-*b*-P3TPy, (b) P3HT-*b*-P3TPy(14/1):PCBPy, (c) P3HT-*b*-P3TPy(10/1):PCBPy, and (d) P3HT-*b*-P3TPy(3/1):PCBPy under as-cast, thermal annealing at 150 °C for 30 min (TA), oDCB solvent annealing for 1 h (SA).

to as-deposited ones. The luminescence quenching is attributed to the fast photoinduced charge transfer between the electron donor and the electron acceptor. For P3HT-*b*-P3TPy:PCBM blends in Figure S6b−d in the Supporting Information, the films under thermal annealing treatment all exhibit the strongest fluorescence quenching, which is well consistent with PL spectra of the P3HT:PCBM system (see Figure S6a in the Supporting Information) upon different annealing treatment. The similar behavior can also be observed in the cases of P3HT-*b*-P3TPy(14/1) and P3HT-*b*-P3TPy(10/1) blended with PCBPy(Figure 3a and 3b), respectively, implying the content of Py mesogen is not high enough to alter the P3HT block dominated photoinduced charge transfer. Nevertheless, for P3HT-*b*-P3TPy(3/1):PCBPy blend (Figure 3c), the situation is just on the opposite. PL spectrum of P3HT-*b*-P3TPy(3/1):PCBPy under SA presents the stronger fluorescence quenching compared to the sample undergoing TA. It can explain that with the amount of Py mesogens increasing, intermolecular interaction between the P3TPy block and PCBPy can be enhanced. And the $\pi-\pi$ interaction of Py mesogens between donor and acceptor under the slow film growth (SA) can be strengthened, consequently leading to more favorable morphology with nanoscale phase separation for more efficient charge transfer. The result is in good agreement with the UV observation. Although P3HT-*b*-P3TPy(3/1):PCBPy system formed more ordered morphology under solvent annealing, the less severe fluorescence quenching of P3HT-*b*-P3TPy(3/1):PCBPy system than that of P3HT-*b*-P3TPy(14/1):PCBPy and P3HT-*b*-P3TPy(10/1):PCBPy is probably due to higher ratio of P3TPy, which possesses the strong light-emitting property.

It is well-known that the intermolecular arrangement and stack could be gained from X-ray diffraction analysis. In order to gain deep insight into the intercalation occurs in P3HT-*b*-P3TPy/PCBPy blend films, the structure of P3HT-*b*-P3TPy/PCBPy films prepared from oDCB solutions were analyzed by XRD measurement. Figure 4A shows the XRD profiles of P3HT-*b*-P3TPy(3/1) pristine film and the blend film undergoing SA. The strong sharp diffraction peak at the low angle (2θ = 5.3°, d_1 = 1.67 nm) corresponds to the arrangement of inter-P3HT aligned by the alkyl side chain, whereas the diffraction peak at high angle implies the $\pi-\pi$ interchain stacking of P3HT. These signals indicate that the hexyl side chains of the P3HT blocks in the P3HT-*b*-P3TPy are oriented normally to the substrate to form an edge-on orientation as the geometry of pure P3HT chains, and the intermolecular $\pi-\pi$ stacking between thiophene rings is parallel to the substrate. Compared to pure P3HT-*b*-P3TPy(3/1) (Figure 4A), pure PCBPy, P3HT-*b*-P3TPy(14/1):PCBPy ,and P3HT-*b*-P3TPy-(10/1):PCBPy blend (see Figure S7 in the Supporting Information), only the diffractogram of the P3HT-*b*-P3TPy-(3/1):PCBPy blend after SA shows an additional weak reflection at 2θ = 2.5°, from which a d_2-spacing of 3.53 nm is obtained. To precisely deduce the possible cooperative packing of the polymer and fullerene, we used density functional theory (DFT) with the Gaussian 09 program package to calculate and simulate the interaction between the polymer and fullerene. The simulated illustration of cooperative assembly structure of P3HT-*b*-P3TPy:PCBPy blend is depicted in Figure 4B. Thus, the d_2-spacing is close to the calculated distance (3.36 nm) from the polymer main chain to the fullerene with the Py groups well interdigitately packed between the P3TPy block and PCBPy.

The UV, PL, and XRD results demonstrate that the SA treatment prolongs the crystallization of the polymers and enable the blend molecules to aggregate together and render a

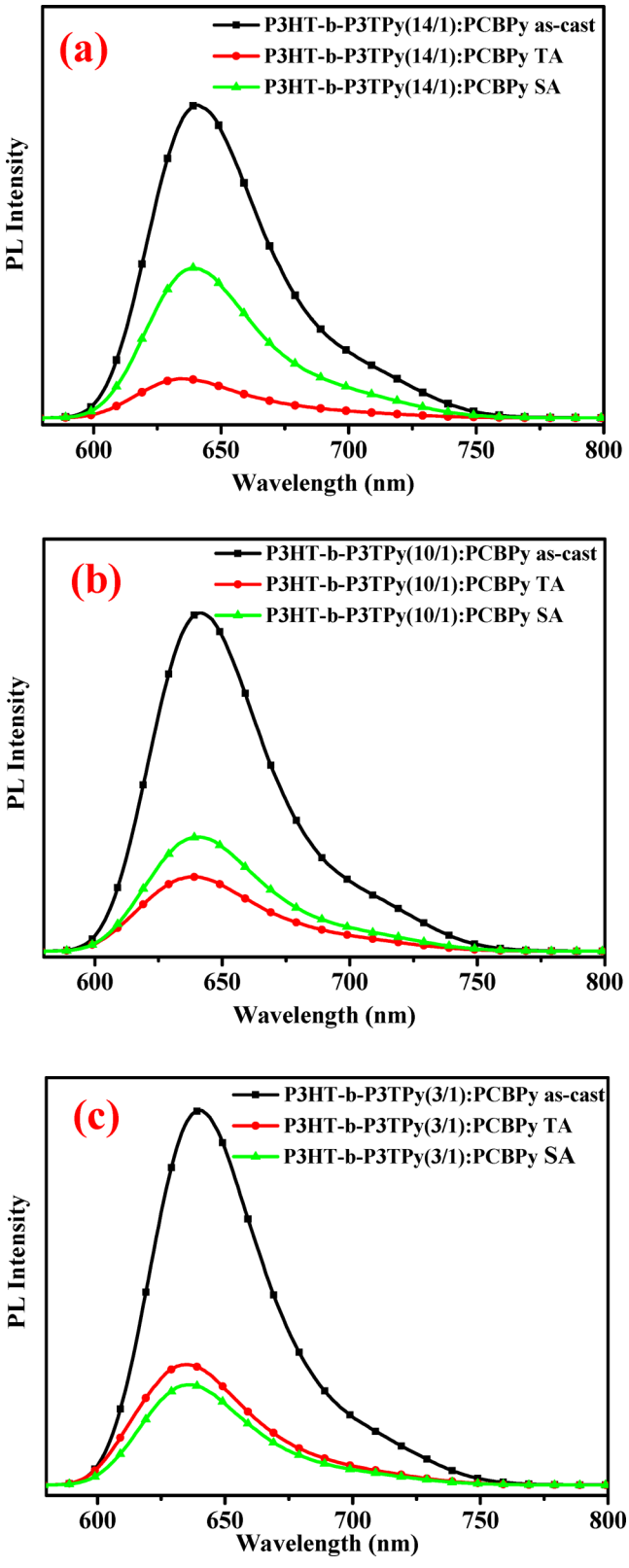

Figure 3. Fluorescence spectra for (a) P3HT-*b*-P3TPy(14/1):PCBPy, (b) P3HT-*b*-P3TPy(10/1):PCBPy, and (c) P3HT-*b*-P3TPy(3/1):PCBPy blend films treated with as-cast, TA, and SA.

more-ordered arrangement. In fact, the assembly microstructure undergoing SA is strongly correlated to the packing competition between polythiophene interchain interaction and Py mesogen interdigitated orientation. The blend with a very

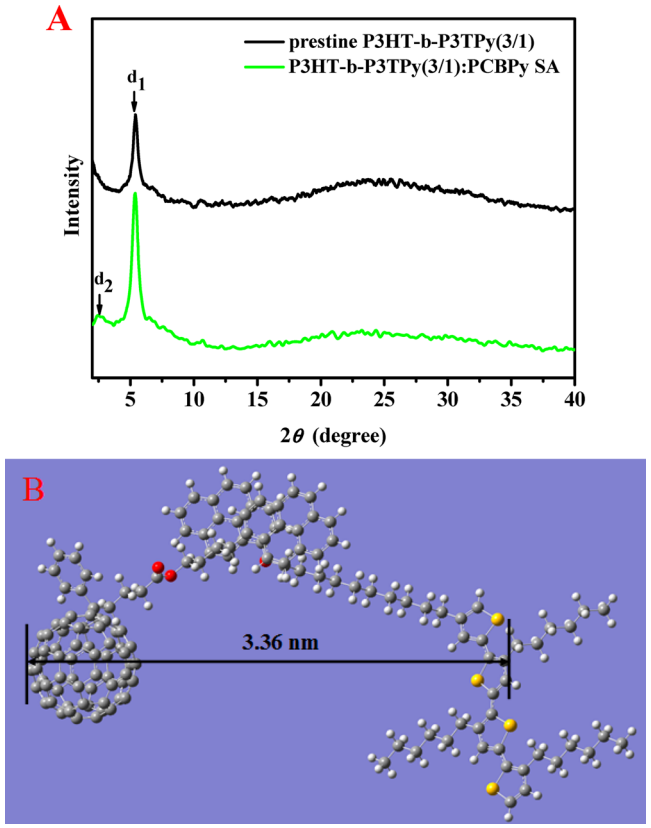

Figure 4. (A) XRD profiles of pure P3HT-*b*-P3TPy(3/1) film and the P3HT-*b*-P3TPy(3/1):PCBPy blend films treated with SA; (B) the simulated illustration of cooperative assembly structure of P3HT-*b*-P3TPy:PCBPy blend.

low content of Py shows only weak $\pi-\pi$ mesogen stacking between the donor and acceptor, and the molecular arrangement is dominated by the polythiophene interchain interaction. Inversely, when the ratio of P3TPy is high enough, the blend film tends to cooperatively assemble into highly ordered microphase separation structure by the interdigitately packed Py mesogen of P3TPy and PCBPy after solvent annealing, which can enlarge surface area for donor/acceptor interfaces and give a bicontinuous pathway for efficient electron transfer. However, too high content of P3TPy block in the copolymer will also disrupt the polythiophene interchain interaction even after long time solvent annealing.[30]

To intuitively determine the microstructure of the P3HT-*b*-P3TPy/PCBPy blends by solvent annealing (SA), AFM are performed on pure P3HT-*b*-P3TPy and the P3HT-*b*-P3TPy/PCBPy blends with oDCB vapor annealing for 1 h. From Figure 5, we can see that the pure P3HT-*b*-P3TPy(14/1) shows a smooth morphology like that of the pure P3HT. However, with the ratio of P3HPy increasing, the P3HT-*b*-P3TPy(3/1) shows random nanowires structure, which may be attributed to the self-assembly of the Py groups. Figure 6 shows the topographic and phase images of the blends films of P3HT-*b*-P3TPy(14/1):PCBPy, P3HT-*b*-P3TPy(10/1):PCBPy and P3HT-*b*-P3TPy(3/1):PCBPy. Phase separation within the P3HT-*b*-P3TPy(3/1):PCBPy appears as distinct domains. Obviously, the surface morphology of P3HT-*b*-P3TPy(14/1):PCBPy and P3HT-*b*-P3TPy(10/1):PCBPy blends is much random, with a rms roughness of 1.93 and 1.33 nm, respectively. Nevertheless, P3HT-*b*-P3TPy(3/1):PCBPy devel-

dx.doi.org/10.1021/am501831z | ACS Appl. Mater. Interfaces 2014, 6, 8115−8123

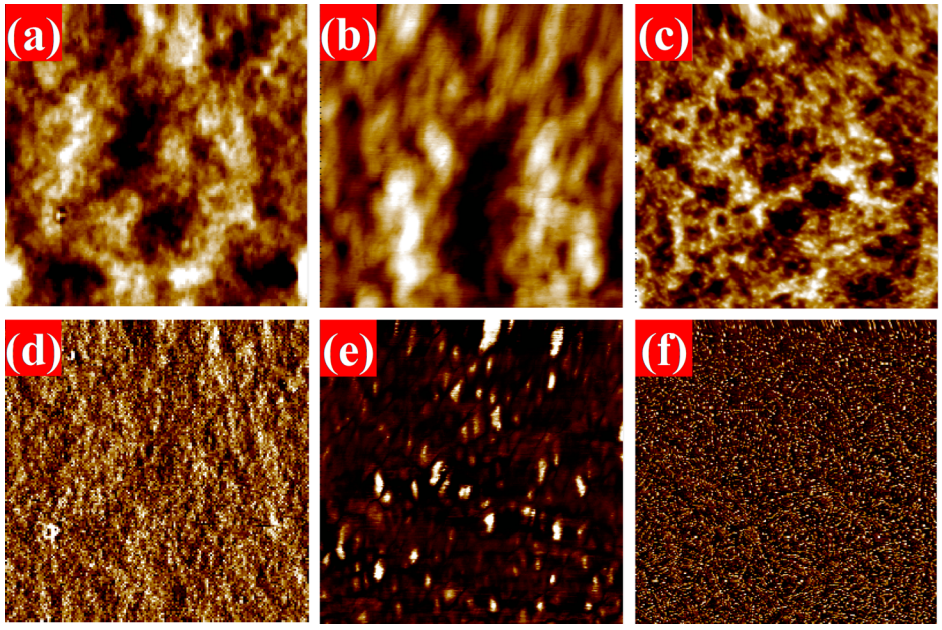

Figure 5. AFM images(3×3 um^2) of spin-coated pure P3HT-*b*-P3TPy films. (a) Topography and (d) phase images of P3HT-*b*-P3TPy(14/1) film with SA treatment; (b) topography and (e) phase images of P3HT-*b*-P3TPy(10/1) film with SA treatment; (c) topography and (f) phase images of P3HT-*b*-P3TPy(3/1) film with SA treatment.

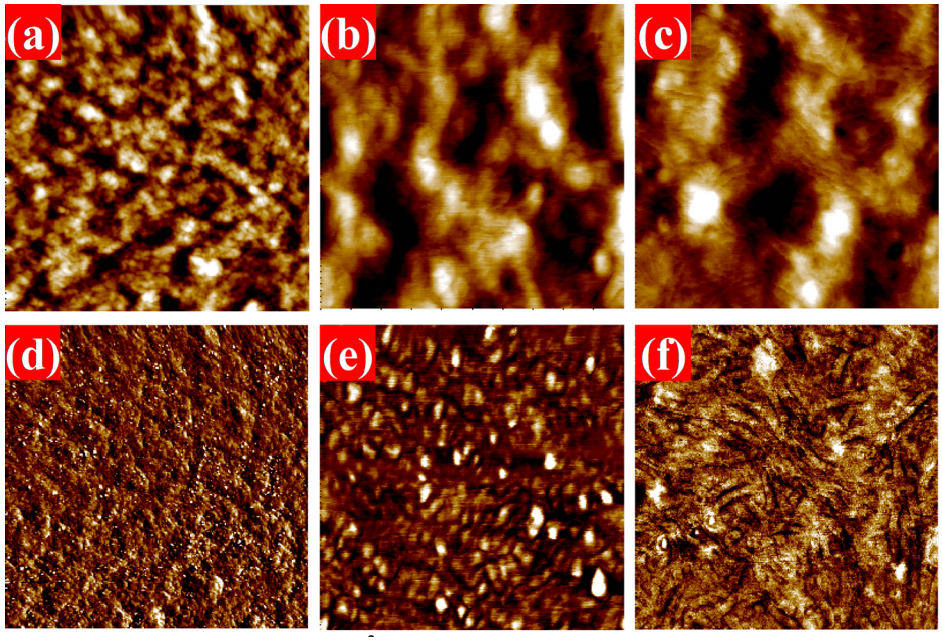

Figure 6. AFM images (3×3 um^2) of spin-coated blend films. (a) Topography and (d) phase images of P3HT-*b*-P3TPy(14/1):PCBPy blend film with SA treatment; (b) topography and (e) phase images of P3HT-*b*-P3TPy(10/1):PCBPy blend film with SA treatment; (c) topography and (f) phase images of P3HT-*b*-P3TPy(3/1):PCBPy blend film with SA treatment.

ops the desirable bulk heterojunction morphology with highly ordered lamellar structure in the blend. The P3HT-*b*-P3TPy(3/1) and PCBPy forms the intimate mixture on the nanoscale, and the phase separation size is very close to the exciton diffusion length, which would remarkable facilitate exciton dissociation. Compared to the random nanowire structure of pure P3HT-*b*-P3TPy(3/1), the small domain size and well-defined nanoscale morphology of P3HT-*b*-P3TPy(3/1):PCBPy illustrate that a strong intermolecular interaction between the P3HT-*b*-P3TPy and PCBPy chains, which is primarily due to the presence of Py mesogens that are capable of forming intermolecular $\pi-\pi$ stacking interaction between P3TPy and PCBPy. As the component of P3TPy block in P3HT-*b*-P3TPy(10/1) and P3HT-*b*-P3TPy(14/1) decreased, the intermolecular interaction between the P3HT-*b*-P3TPy and PCBPy has been greatly weakened. The related DSC results of the three diblock copolymers P3HT-*b*-P3TPy, PCBPy and the blends have been shown in Figure S8 in the Supporting Information. The P3HT-*b*-P3TPy:PCBPy blend was dissolved in the oDCB. After the solvent evaporated, the drying solids of the blends are obtained for DSC measurement. The three diblock copolymers show two characteristic melting peaks of

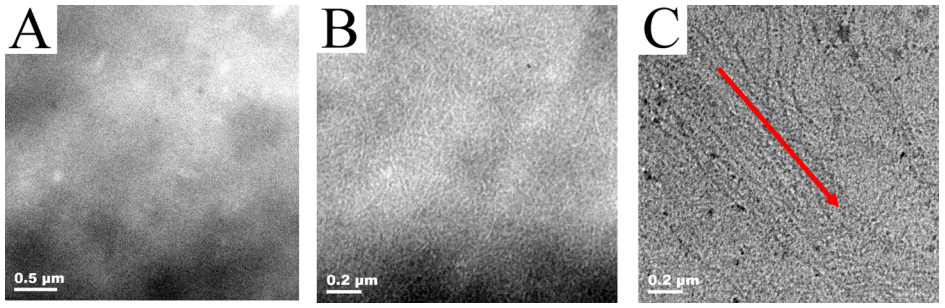

Figure 7. TEM images of nanostructure assembled from (A) P3HT-*b*-P3TPy(14/1):PCBPy, (B) P3HT-*b*-P3TPy(10/1), and (C) P3HT-*b*-P3TPy(3/1):PCBPy blend films prepared by SA treatment.

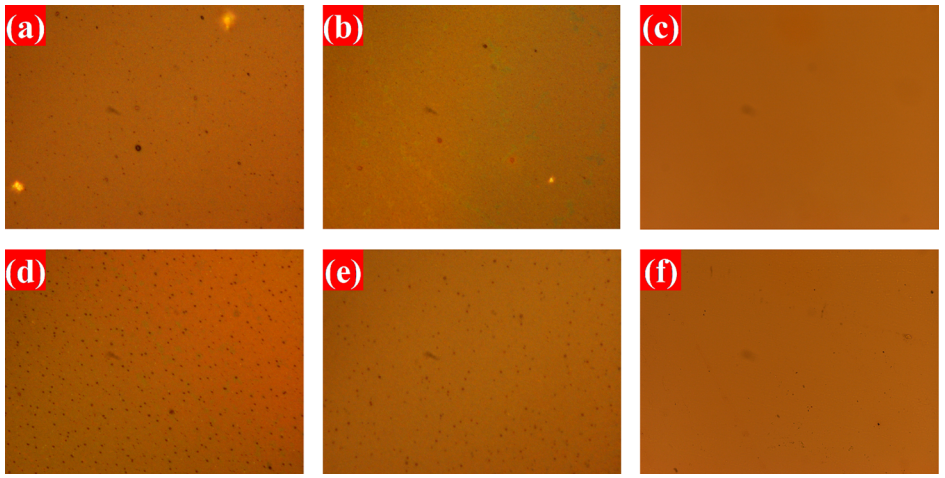

Figure 8. Optical microscopy images of (a, d) P3HT-*b*-P3TPy(14/1):PCBPy (1:1 wt %) blends, (b, e) P3HT-*b*-P3TPy(10/1):PCBPy (1:1 wt %) blends, and (c, f) P3HT-*b*-P3TPy(3/1):PCBPy (1:1 wt %) blends with thermal annealing at 150 °C. The annealing time for a–c is 2 h, and that for d–f is 6 h.

diblock copolymers (see Figure S8A in the Supporting Information), compared to the pure P3HT. The peak at low temperature belongs to the P3HT block, while the peak at high temperature is assigned to the P3TPy block. With the ratio of P3TPy block increasing, the peak at high temperature becomes stronger. But from the Figure S8B in the Supporting Information, we can see clearly that the melting transition peaks of the P3TPy block at the three copolymers all disappear, indicating that interaction has happened between the P3TPy block and PCBPy, which limits the crystallization of the P3TPy block and PCBPy. Thus, the DSC analysis is consistent with the AFM results.

The cooperative assembly of P3HT-*b*-P3TPy and PCBPy by solvent annealing has also been confirmed by TEM. As shown in Figure 7, the P3HT-*b*-P3TPy(14/1):PCBPy blend film forms homogeneously morphology with isotropic distribution of donor and acceptor, which is very similar to the P3HT:PCBM blend.[33] As the weight ratio of P3TPy and P3HT block increases to 1:10, a large amount of nanowires are observed in P3HT-*b*-P3TPy(10/1):PCBPy blend film, because of the strong assembly nature of Py-functionalized block copolymers. Further increasing the content of P3TPy block, these nanowires are orientated to highly ordering lamellar structure. It is worth noting that the driven force behind the assembled nanowires is related to the strong $\pi-\pi$ interactions of pyrene moiety in both donor and acceptor. The domain size of lamellar structure is calculated to be 10–20 nm, which is also in accordance with the AFM results.

The morphological stability of the blend is a crucial factor for practical PSC application. Most BHJ structures usually suffer from damage during prolonged exposure to operation conditions, because of the fullerene diffusion and phase separation caused by the heat. Polarizing optical micrographic images of P3HT-*b*-P3TPy/PCBPy (1:1 wt %) under harsh thermal annealing conditions (2 h, 6 h) at 150 °C describe the function of cooperative assembly on the morphology stability. The samples are prepared on the SA treatment before the thermal treatment. The images are shown in Figure 8. It is clearly observed that large aggregates of PCBPy appears and gradually grows to ball-like crystals throughout the P3HT-*b*-P3TPy(14/1):PCBPy films after annealing for 2 and 6 h. Similar phenomenon happens to the P3HT-*b*-P3TPy(10/1):PCBPy films, but with less formed PCBPy crystallites. In sharp contrast, for P3HT-*b*-P3TPy(3/1):PCBPy, thermal annealing can not induce the large aggregation of PCBPy, and the morphology almost keeps unchanged undergoing thermal annealing for 2h, even after 6 h of continuous annealing. This suggests that the cooperative assembly between P3HT-*b*-P3TPy and PCBPy can effectively suppress the PCBPy diffusion and phase separation, and stabilize the blend morphology.

CONCLUSIONS

In this study, Py-functionalized diblock copolymers P3HT-*b*-P3TPy were successfully synthesized by Grignard metathesis (GRIM) reaction. And the fullerene derivative PCBPy

containing Py was obtained via esterification reaction. The strong $\pi-\pi$ stacking interactions of Py mesogens interdigitated between PCBPy and P3TPy segment result in a preferential distribution of the fullerenes within the P3TPy domains and a desirable nanostructured D/A interpenetrated network. Under SA treatment, the P3HT-*b*-P3TPy(3/1):PCBPy blend film can cooperative self-assemble into highly ordered nanowires which can enlarge surface area for donor/acceptor interfaces and give a bicontinuous pathway for efficient electron transfer. Because of the strong $\pi-\pi$ stacking interactions of Py mesogens, morphological stability has also been greatly improved. Therefore, this study paves a facile way for the development of stable and well-defined BHJ nanomorphology by mesogen-induced cooperative assembly of donor and acceptor via intermolecular noncovalent $\pi-\pi$ interactions.

■ ASSOCIATED CONTENT

Supporting Information

Text giving the experimental details, instrumentation, and characterization. This material is available free of charge via the Internet at http://pubs.acs.org/.

■ AUTHOR INFORMATION

Corresponding Author

*E-mail: ywchen@ncu.edu.cn. Tel.: +86 791 83969562. Fax: +86 791 83969561.

Notes

The authors declare no competing financial interest.

■ ACKNOWLEDGMENTS

This work was supported by the National Natural Science Foundation of China (51273088 and 51263016).

■ REFERENCES

(1) Peet, J.; Heeger, A. J.; Bazan, G. C. Plastic Solar Cells: Self-Assembly of Bulk Heterojunction Nanomaterials by Spontaneous Phase Separation. *Acc. Chem. Res.* **2009**, *42*, 1700−1708.

(2) Gunes, S.; Neugebauer, H.; Sariciftci, N. S. Conjugated Polymer-Based Organic Solar Cells. *Chem. Rev.* **2007**, *107*, 1324−1338.

(3) He, M.; Qiu, F.; Lin, Z. Conjugated Rod-Coil and Rod-Rod Block Copolymers for Photovoltaic Applications. *J. Mater. Chem.* **2011**, *21*, 17039−17048.

(4) Woo, C. H.; Thompson, B. C.; Kim, B. J.; Toney, M. F.; Fréchet, J. M. The Influence of Poly(3-hexylthiophene) Regioregularity on Fullerene-Composite Solar Cell Performance. *J. Am. Chem. Soc.* **2008**, *130*, 16324−16329.

(5) Li, G.; Shrotriya, V.; Huang, J.; Yao, Y.; Moriarty, T.; Emery, K.; Yang, Y. High-Efficiency Solution Processable Polymer Photovoltaic Cells by Self-Organization of Polymer Blends. *Nat. Mater.* **2005**, *4*, 864−868.

(6) Zhang, Y.; Yip, H. L.; Acton, O.; Hau, S. K.; Huang, F.; Jen, A. K. Y. A Simple and Effective Way of Achieving Highly Efficient and Thermally Stable Bulk-Heterojunction Polymer Solar Cells Using Amorphous Fullerene Derivatives as Electron Acceptor. *Chem. Mater.* **2009**, *21*, 2598−2600.

(7) Ma, W.; Yang, C.; Gong, X.; Lee, K.; Heeger, A. J. Thermally Stable, Efficient Polymer Solar Cells with Nanoscale Control of the Interpenetrating Network Morphology. *Adv. Funct. Mater.* **2005**, *15*, 1617.

(8) Kim, J. Y.; Kim, S. H.; Lee, H. H.; Lee, K.; Ma, W.; Gong, X.; Heeger, A. J. New Architecture for High-Efficiency Polymer Photovoltaic Cells Using Solution-Based Titanium Oxide as an Optical Spacer. *Adv. Mater.* **2006**, *18*, 572−576.

(9) Pettersson, L. A.; Roman, L. S.; Inganas, O. Modeling Photocurrent Action Spectra of Photovoltaic Devices Based on Organic Thin Films. *J. Appl. Phys.* **1999**, *86*, 487−496.

(10) Halls, J. J. M.; Pichler, K.; Friend, R. H.; Moratti, S. C.; Holmes, A. B. Exciton Diffusion and Dissociation in a Poly(p-phenylenevinylene)/C_{60} Heterojunction Photovoltaic Cell. *Appl. Phys. Lett.* **1996**, *68*, 3120−3122.

(11) Chirvase, D.; Parisi, J.; Hummelen, J. C.; Dyakonov, V. Influence of Nanomorphology on the Photovoltaic Action of Polymer−Fullerene Composites. *Nanotechnology* **2004**, *15*, 1317−1323.

(12) Nguyen, L. H.; Hoppe, H.; Erb, T.; Guenes, S.; Gobsch, G.; Sariciftci, N. S. Effects of Annealing on the Nanomorphology and Performance of Poly(alkylthiophene):Fullerene Bulk-Heterojunction Solar Cells. *Adv. Funct. Mater.* **2007**, *17*, 1071−1078.

(13) Zhao, Y.; Xie, Z.; Qu, Y.; Geng, Y.; Wang, L. Solvent-Vapor Treatment Induced Performance Enhancement of Poly(3-hexylthiophene):Methanofullerene Bulk-Heterojunction Photovoltaic Cells. *Appl. Phys. Lett.* **2007**, *90*, 043504.

(14) Janssen, G.; Aguirre, A.; Goovaerts, E.; Vanlaeke, P.; Poortmans, J.; Manca, J. Optimization of Morphology of P3HT/PCBM Films for Organic Solar Cells: Effects of Thermal Treatments and Spin Coating Solvents. *Eur. Phys. J.: Appl. Phys.* **2007**, *37*, 287−290.

(15) Di Nuzzo, D.; Aguirre, A.; Shahid, M.; Gevaerts, V. S.; Meskers, S. C.; Janssen, R. A. Improved Film Morphology Reduces Charge Carrier Recombination into the Triplet Excited State in a Small Bandgap Polymer-Fullerene Photovoltaic Cell. *Adv. Mater.* **2010**, *22*, 4321−4324.

(16) Loewe, R. S.; Khersonsky, S. M.; McCullough, R. D. A Simple Method to Prepare Head-to-Tail Coupled, Regioregular Poly(3-alkylthiophenes) Using Grignard Metathesis. *Adv. Mater.* **1999**, *11*, 250−253.

(17) Loewe, R. S.; Ewbank, P. C.; Liu, J.; Zhai, L.; McCullough, R. D. Regioregular, Head-to-Tail Coupled Poly(3-alkylthiophenes) Made Easy by the GRIM Method: Investigation of the Reaction and the Origin of Regioselectivity. *Macromolecules* **2001**, *34*, 4324−4333.

(18) Brinkmann, M.; Wittmann, J. C. Orientation of Regioregular Poly(3-hexylthiophene) by Directional Solidification: A Simple Method to Reveal the Semicrystalline Structure of a Conjugated Polymer. *Adv. Mater.* **2006**, *18*, 860−863.

(19) Crossland, E. J.; Tremel, K.; Fischer, F.; Rahimi, K.; Reiter, G.; Steiner, U.; Ludwigs, S. Anisotropic Charge Transport in Spherulitic Poly(3-hexylthiophene) Films. *Adv. Mater.* **2012**, *24*, 839−844.

(20) Lee, E.; Hammer, B.; Kim, J. K.; Page, Z.; Emrick, T.; Hayward, R. C. Hierarchical Helical Assembly of Conjugated Poly(3-hexylthiophene)-block-poly(3-triethylene glycol thiophene) Diblock Copolymers. *J. Am. Chem. Soc.* **2011**, *133*, 10390−10393.

(21) Yang, C.; Lee, J. K.; Heeger, A. J.; Wudl, F. Well-Defined Donor−Acceptor Rod−Coil Diblock Copolymers Based on P3HT Containing C_{60}: the Morphology and Role as a Surfactant in Bulk-Heterojunction Solar Cells. *J. Mater. Chem.* **2009**, *19*, 5416−5423.

(22) Lin, Y.; Lim, J. A.; Wei, Q.; Mannsfeld, S. C.; Briseno, A. L.; Watkins, J. J. Cooperative Assembly of Hydrogen-Bonded Diblock Copolythiophene/Fullerene Blends for Photovoltaic Devices with Well-Defined Morphologies and Enhanced Stability. *Chem. Mater.* **2012**, *24*, 622−632.

(23) Kim, H. J.; Han, A. R.; Cho, C. H.; Kang, H.; Cho, H. H.; Lee, M. Y.; Fréchet, J. M. J.; Oh, J. H.; Kim, B. J. Solvent-Resistant Organic Transistors and Thermally Stable Organic Photovoltaics Based on Cross-Linkable Conjugated Polymers. *Chem. Mater.* **2012**, *24*, 215−221.

(24) Yao, K.; Chen, L.; Li, F.; Wang, P.; Chen, Y. Cooperative Assembly Donor-Acceptor System Induced by Intermolecular Hydrogen Bonds Leading to Oriented Nanomorphology for Optimized Photovoltaic Performance. *J. Phys. Chem. C* **2012**, *116*, 714−721.

(25) Fang, H.; Wang, S.; Xiao, S.; Yang, J.; Li, Y.; Shi, Z.; Li, H.; Liu, H.; Xiao, S.; Zhu, D. Three-Point Hydrogen Bonding Assembly between a Conjugated PPV and a Functionalized Fullerene. *Chem. Mater.* **2003**, *15*, 1593−1597.

(26) Fang, H.; Shi, Z.; Li, Y.; Xiao, S.; Li, H.; Liu, H.; Zhu, D. Self-Assembly of a Derivated PPV and a Functionnalized Fullerene by Hydrogen Bonding. *Synth. Met.* **2003**, *135*, 843−844.
(27) Hsu, S. L.; Chen, C. M.; Cheng, Y. H.; Wei, K. H. New Carbazole-Based Conjugated Polymers Containing Pyridylvinyl Thiophene Units for Polymer Solar Cell Applications: Morphological Stabilization Through Hydrogen Bonding. *J. Polym. Sci., Part A: Polym. Chem.* **2011**, *49*, 603−611.
(28) Lai, Y. C.; Ohshimizu, K.; Takahashi, A.; Hsu, J. C.; Higashihara, T.; Ueda, M.; Chen, W. C. Synthesis of All-Conjugated Poly(3-hexylthiophene)-block-poly(3-(4′-(3″,7″-dimethyloctyloxy)-3′-pyridinyl)thiophene) and Its Blend for Photovoltaic Applications. *J. Polym. Sci., Part A: Polym. Chem.* **2011**, *49*, 2577−2587.
(29) Li, F.; Yager, K. G.; Dawson, N. M.; Yang, J.; Malloy, K. J.; Qin, Y. Complementary Hydrogen Bonding and Block Copolymer Self-Assembly in Cooperation toward Stable Solar Cells with Tunable Morphologies. *Macromolecules* **2013**, *46*, 9021−9031.
(30) Chen, X.; Chen, L.; Yao, K.; Chen, Y. Self-Assembly of Diblock Polythiophenes with Discotic Liquid Crystals on Side Chains for the Formation of a Highly Ordered Nanowire Morphology. *ACS Appl. Mater. Interfaces* **2013**, *5*, 8321−8328.
(31) Kuila, B. K.; Chakraborty, C.; Malik, S. A Synergistic Coassembly of Block Copolymer and Fluorescent Probe in Thin Film for Fine-Tuning the Block Copolymer Morphology and Luminescence Property of the Probe Molecules. *Macromolecules* **2013**, *46*, 484−492.
(32) Sehgal, R. K.; Kumar, S. A Simple Preparation of 1-Hydroxypyrene. *Org. Prep. Proced. Int.* **1989**, *21*, 223−225.
(33) Tsoi, W. C.; Spencer, S. J.; Yang, L.; Ballantyne, A. M.; Nicholson, P. G.; Turnbull, A.; Shard, A. G.; Murphy, G. E.; Bradley, D. D. C.; Nelson, J.; Kim, J. S. Effect of Crystallization on the Electronic Energy Levels and Thin Film Morphology of P3HT:PCBM Blends. *Macromolecules* **2011**, *44*, 2944−2952.